

INTERNATIONAL SOCIETY FOR SOIL MECHANICS AND GEOTECHNICAL ENGINEERING



This paper was downloaded from the Online Library of the International Society for Soil Mechanics and Geotechnical Engineering (ISSMGE). The library is available here:

<https://www.issmge.org/publications/online-library>

This is an open-access database that archives thousands of papers published under the Auspices of the ISSMGE and maintained by the Innovation and Development Committee of ISSMGE.

Numerical investigation of hydraulic fracture in saturated cohesive body

Numérique Recherche sur la rupture hydraulique dans le corps cohésif saturé

Seyed Amirodin Sadrnejad

Dept. of Civil Eng., K.N.Toosi University of Tech., Teheran, Iran

E-mail:sadrnejad@hotmail.com

ABSTRACT

Hydraulic fracturing, is defined as the process of initiation and propagation of cracks due to fluid pressure at relatively high flow rates in cohesive soil. Fractures in cohesive earth layers are desired for a variety of reasons, including enhanced oil and gas recovery, re-injection of drilling or other environmentally sensitive wastes, measurement of in situ stresses, geothermal energy recovery, and enhanced well water production. These fractures can range in size from a few meters to hundreds of metres and their cost is often a significant portion of the total development cost. In locations where the in situ stress field, including the directions, is known and the oil well-bore is aligned with one of the far-field principal stresses, the hydraulic fracture geometry can be predicted and controlled with reasonable accuracy. Numerical simulations and an accurate elastic-plastic model may be used to evaluate and predict the location in three dimension medium, orientation and extent of hydraulic fractures.

Efficient numerical simulation of 3-D hydraulic fracturing requires two key components. The first is a capability for representing and visualizing fracture geometries and the second is a method to solve the highly non-linear coupling between the equations of fluid flow in the fracture and the deformation and propagation of the fracture. The first component may be partitioned into several sub-components, including geometrical and topological solid modeling tools, routines to model geometry and topology changes for fracture propagation, visualization of historical response information, and analysis control information. The second component consists of a stress analysis procedure, fluid flow simulation capabilities, and a method for coupling the solid skeleton structure response with the fluid flow, including rules for determining hydraulic fracture propagation and probable internal mechanism of widening/closing and sliding bands.

In this paper a multi-plane elastic-plastic model developed as a simulator that includes all of these components for modeling fully 3-D, hydraulic fracture propagation. This simulated framework treats hydraulic fracturing as quasi-static process, and the solution consists of a series of snapshots in time of the fracture geometry, fluid pressures, and crack opening displacements.

RÉSUMÉ

La rupture hydraulique, est définie comme processus de déclenchement et de propagation des fissures dues à la pression du liquide aux débits relativement élevés dans le sol cohérent. Des ruptures dans des couches cohésives de la terre sont désirées pour une variété de raisons, y compris le rétablissement augmenté de pétrole et de gaz, l're-injection du forage ou autre pertes dans l'environnement sensibles, mesure des efforts in situ, géothermique rétablissement d'énergie, et production augmentée d'eau de puits. Ces ruptures peuvent s'étendre dans la taille de quelques mètres aux centaines de distribue et leur coût est souvent a partie significative de tout le coût de développement. Dans les endroits dans où le champ de contrainte de situ, y compris les directions, est connu et le puits d'huile est aligné avec un des principaux efforts de loin-champ, la rupture hydraulique la géométrie peut être prévue et commandée avec l'exactitude raisonnable. Numérique des simulations et un modèle précis de élastique-plastique peuvent être employés pour évaluer et prévoyez l'endroit dans le milieu, l'orientation et l'ampleur de trois dimensions de ruptures hydrauliques.

La simulation numérique efficace de la rupture 3-D hydraulique exige la clef deux composants. Le premier est des possibilités pour représenter et visualiser la rupture les geometries et la seconde est une méthode pour résoudre l'accouplement fortement non linéaire entre les équations du flux de fluide dans la rupture et la déformation et propagation de la rupture. Le premier composant peut être divisé dans plusieurs sous-composants, y compris modeler plein géométrique et topologique outils, routines pour modeler la géométrie et des changements de topologie pour la rupture propagation, visualisation d'information historique de réponse, et analyse paramètres. Le deuxième composant se compose d'une analyse d'effort procédé, possibilités de simulation de flux de fluide, et une méthode pour coupler réponse squelettique pleine de structure avec le flux de fluide, y compris des règles pour détermination de la propagation hydraulique de rupture et du mécanisme interne probable de bandes de widening/fermeture et de glissement.

En cet article un modèle de élastique-plastique d'multi-avion développé comme simulateur cela inclut tous ces composants pour modeler entièrement 3-D, rupture hydraulique propagation. Ce cadre simulé traite la rupture hydraulique As le processus quasistatique, et la solution se compose d'une série d'instantanés dedans période de la géométrie de rupture, des pressions du liquide, et des déplacements d'ouverture de fente.

1 INTRODUCTION

Hydro-fracturing is often less effective for deviated well-bores as compared to deviated to traditional vertical wells. This feature may be attributed to a poor understanding of the mechanisms of fracture initiation and propagation from a

deviated well-bore. The stress state that is generated around an inclined well-bore may be considered that the fracture propagates with a complex geometry (Weijers and de Pater, 1992, Abass et al., 1996). This complex stress state associated with fracture geometry can limit the fracture width at the well-

bore and hinder the injection of proppant into the fracture leading to fracture premature screen-out (Soliman et al., 1996).

According to the proposed models and frameworks, in addition to inadequate modeling of fracture geometry many of the current hydraulic fracturing simulations do not predict the correct well-bore fluid pressure or fracture geometry even for planar fractures (Van den Hoek et al., 1993).

A multi-plane based model capable of predicting the behavior of porous material on the basis of sliding mechanisms and elastic behavior of particles has been already presented (Sadrejad, 1993).

2 MULTI-LAMINATE MODEL

The task of representing the overall stress tensor in terms of micro level stresses and the condition, number and magnitude of contact forces has long been the aim of numerous researchers (Christofferson, et. al., 1981, Konishi, 1978, Nemat-Nasser, et. al., 1983). The first multilaminar model presented by Zienkiewicz et. al. 1977. A multilaminar model for granular material was developed by Sadrejad, et al. 1987, and Sadrejad, 1990. Also, a micro-plane model was developed by Bazant, et. al, 1983.

Multi-plane framework defined by small continuum structural units formed as an assemblage of particles and voids filling infinite spaces between the sampling planes, has appropriately justified the contribution of interconnection forces in overall macro-mechanics. Plastic deformations are assumed to occur due to sliding as shearing, separation/closing of the boundaries as volume change. Figure 1 shows the arrangement of artificial polyhedron simulated by real soil grains. The polyhedrons are roughly created by 13 sliding planes passing through each point in medium. The location of tip heads of normal to the planes defining corresponding direction cosines are shown on the surface of unit radius sphere.

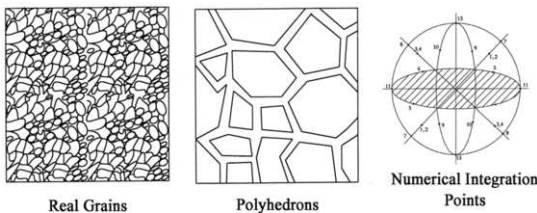


Figure 1 polyhedrons, and sampling points

3 CONSTITUTIVE EQUATIONS

The increment of elastic strain ($d\epsilon_e$) is related to the increments of effective stress ($d\sigma$) by:

$$d\epsilon_e = [De]^{-1} d\sigma \quad (1)$$

For the soil mass, the overall stress-strain increments relation, to obtain plastic strain increments ($d\epsilon_p$), is expressed as:

$$d\epsilon_p = C_p \cdot d\sigma \quad (2)$$

Direction cosines of integration points									Weights M_i	
ℓ_1^1	m_1^1	n_1^1	ℓ_1^2	m_1^2	n_1^2	ℓ_1^3	m_1^3	n_1^3		
$+\sqrt{1/3}$	$+\sqrt{1/3}$	$+\sqrt{1/3}$	$+\sqrt{1/6}$	$+\sqrt{1/6}$	$-\sqrt{2/3}$	$-\sqrt{1/2}$	$+\sqrt{1/2}$	0	27/840	Planes 1, 2, 3 & 4
$+\sqrt{1/3}$	$-\sqrt{1/3}$	$+\sqrt{1/3}$	$+\sqrt{1/6}$	$-\sqrt{1/6}$	$-\sqrt{2/3}$	$-\sqrt{1/2}$	$+\sqrt{1/2}$	0	27/840	
$-\sqrt{1/3}$	$+\sqrt{1/3}$	$+\sqrt{1/3}$	$+\sqrt{1/6}$	$+\sqrt{1/6}$	$-\sqrt{2/3}$	$-\sqrt{1/2}$	$+\sqrt{1/2}$	0	27/840	
$+\sqrt{1/3}$	$+\sqrt{1/3}$	$-\sqrt{1/3}$	$+\sqrt{1/6}$	$+\sqrt{1/6}$	$-\sqrt{2/3}$	$+\sqrt{1/2}$	$-\sqrt{1/2}$	0	27/840	Planes 5 & 6
$+\sqrt{1/3}$	$-\sqrt{1/3}$	$-\sqrt{1/3}$	$+\sqrt{1/6}$	$-\sqrt{1/6}$	$-\sqrt{2/3}$	$+\sqrt{1/2}$	$-\sqrt{1/2}$	0	27/840	
$-\sqrt{1/3}$	$+\sqrt{1/3}$	$-\sqrt{1/3}$	$+\sqrt{1/6}$	$-\sqrt{1/6}$	$-\sqrt{2/3}$	$+\sqrt{1/2}$	$-\sqrt{1/2}$	0	27/840	
$+\sqrt{1/3}$	$+\sqrt{1/3}$	0	$+\sqrt{1/6}$	$+\sqrt{1/6}$	0	0	0	1	32/840	Planes 7, 8, 9 & 10
$+\sqrt{1/3}$	$-\sqrt{1/3}$	0	$+\sqrt{1/6}$	$-\sqrt{1/6}$	0	0	0	1	32/840	
$-\sqrt{1/3}$	$+\sqrt{1/3}$	0	$+\sqrt{1/6}$	$+\sqrt{1/6}$	0	0	0	1	32/840	
$+\sqrt{1/3}$	0	$+\sqrt{1/3}$	$+\sqrt{1/6}$	0	$+\sqrt{1/6}$	0	1	0	32/840	Planes 11, 12 & 13
$+\sqrt{1/3}$	0	$-\sqrt{1/3}$	$+\sqrt{1/6}$	0	$-\sqrt{1/6}$	0	1	0	32/840	
$-\sqrt{1/3}$	0	$+\sqrt{1/3}$	$+\sqrt{1/6}$	0	$+\sqrt{1/6}$	0	1	0	32/840	
0	$+\sqrt{1/3}$	$+\sqrt{1/3}$	0	$-\sqrt{1/6}$	$+\sqrt{1/6}$	1	0	0	32/840	
0	$+\sqrt{1/3}$	$-\sqrt{1/3}$	0	$-\sqrt{1/6}$	$-\sqrt{1/6}$	1	0	0	32/840	
0	0	0	0	0	0	1	0	0	40/840	
0	0	0	0	0	0	0	0	1	40/840	
0	0	0	0	0	0	0	0	0	40/840	

Figure 2 Direction cosines, weight coefficients, Demonstration of 13 planes

where, C_p is plastic compliance matrix. Clearly, it is expected that all effects of plastic behavior be included in C_p . To find out C_p , the constitutive equations for a typical slip plane must be considered in calculations. Consequently, the appropriate summation of all provided compliance matrices corresponding to considered slip planes yields overall C_p , therefore, strain increment at each stress increment is calculated as follows:

$$d\epsilon^p = \frac{1}{n} \sum_{i=1}^n W_i [L\epsilon]^T C_i^p [L\sigma] d\sigma' \quad (6)$$

where, $L\epsilon$ and $L\sigma$ are transformation matrices for strain and stresses, respectively and n is number of planes.

A sampling plane is defined as a boundary surface that is a contacting surface between two structural units of polyhedral blocks. These structural units are parts of an heterogeneous continuum and for simplicity they are defined as a full homogeneous and isotropic material. Therefore, all heterogeneities behaviour are supposed to appear in inelastic behaviour of corresponding slip planes.

In this constitutive formulation, the yield criterion is defined by the absolute ratio of shear stress (τ) to the normal effective stress (σ_{ni}) on i th sampling plane. The simplest form of yield function i.e. a straight line on τ versus σ_{ni} space is adopted. As the ratio τ/σ_{ni} increases, the yield surface represented by the straight line, rotates anti-clock-wise due to hardening and approaches Mohr-Coulomb's failure line and finally failure on corresponding plane takes place.

The equation of yield function is formulated as follows:

$$F_i(\bar{\tau}_i, \bar{\sigma}_{ni}, \eta_i) = \bar{\tau}_i - C_i' - \eta_i \bar{\sigma}_{ni} \quad (4)$$

where, $\eta_i = \tan(\alpha_i)$ is a hardening parameter and assumed as a hyperbolic function of plastic shear strain on the i th plane. α_i is the slope of yield line and C_i' is cohesion of soil.

The plastic potential function is stated in terms of $\bar{\tau}_i$ and $\bar{\sigma}_{ni}$ for the τ versus σ_{ni} space as follows:

$$\psi(\bar{\tau}_i, \bar{\sigma}_{ni}) = \bar{\tau}_i - C_i' + \eta_c \cdot \bar{\sigma}_{ni} \cdot \log(\bar{\sigma}_{ni} / \bar{\sigma}_{nic}) \quad (5)$$

where, η_c is the slope of critical state line and $\bar{\sigma}_{nic}$ is the value of effective normal stress the i th plane when $\bar{\tau}_i = C_i'$

$$C_i^p = \{1/Hp_i\} \cdot \{\partial\psi_i/\partial\sigma_i\} \{\partial F_i/\partial\sigma_i\} \quad (6)$$

C_{pi} is a 2x2 matrix and as a whole, represent the plastic resistance corresponds to the i th active plane in plasticity and must be summed up as the contribution of this plane with the others after transforming into 6x6 size in global coordinate. Accordingly, the conceptual numerical integration of multilaminate framework presents the following summation for computing C_p .

$$C^p = 4\Pi \cdot \sum_{i=1}^n W_i \cdot L^T C_i^p L \quad (7)$$

where W_i are the weight coefficients and C_p is the global plastic compliance matrix corresponding to a single point in the medium and L is transformation matrix for the corresponding plane. n is the employed number of planes.

4 PORE PRESSURE AND HYDRAULIC FRACTURE

Pore water pressure can be divided into static and excessive water pressures, and pore spaces are assumed to be saturated with water. There are many different cases in structures made of saturated soil that built up excess pore water pressure overcame the local tensile strength and hydraulic fracture took place on a certain orientation. Many investigations presented different pore pressure causing hydraulic fracture. Komakpanah (1994) experimentally carried out a relation between pore pressure and soil strength parameters as follows:

$$P_f = (1 + \sin \phi_u) \sigma_h + C_u \cos \phi_u \quad (8)$$

P_f is pore pressure, ϕ_u , σ_h and C_u are internal friction angle, lateral stress and cohesion in saturated soil respectively. Medeiros et al. (1996) also showed that in cohesive soil, hydraulic fracture takes place when the normal effective stress on certain orientation is less than tensile strength at that orientation. However, in a general case, it could be claimed that where ever through the medium the total pore water pressure exceeds the existing tensile strength, hydraulic fracture may take place along the orientation that satisfy the minimum energy level conditions.

Proper volumetric coupling based on using average water/solid grain bulk modulus yields an analytical model for excess pore pressure near crack front. However, the general solution for water flow in vicinity of the tip of hydraulic fracture propagating in an impermeable solid is a certain steady state while the solid skeleton behavior is elastic-plastic. Furthermore, according to the investigation carried out by Pak, et al. 1999, hydraulic fracture may occur in three modes denoted by nodes 1, 2 and 3 for tensile separation as in plane shearing and out of plane tearing, respectively. However, in undrained condition induced by fast occurrence of hydraulic fracture, no leak-off may take place during hydraulic fracturing and the mode of fracture is most likely tensile.

5 SAN-FERNANDO DAM FAILURE

This dam that is located near Los-Angeles city, was failed by 6.6 richter earthquake on 9th-Feb.-Seed et al.1971, Lee et al. 1975. According to calibration of model results with two test

results on non-cohesive and cohesive samples the following parameters are obtained. For cohesive soil used in core:

$E=9000 \text{ KPa.}$, $\nu=0.3$, $\phi=20^\circ$, $\eta c=0.98 \text{ Tan}\phi$, $C'=1 \text{ KPa.}$, $A=0.001, \gamma=15 \text{ KN/m}^3$.

For non-cohesive soil used in dam body except core:

$E=9667 \text{ KPa.}$, $\nu=0.377$, $\phi=32.62^\circ$, $\eta c=0.75 \text{ Tan}\phi$, $C'=0$, $A=0.002, \gamma=16.69 \text{ KN/m}^3$.

The dam height is 50m, the length is 275m, the height of water at the time of earthquake was 36m, and the aim of this computation is elastic-plastic behavior during 12 seconds of earthquake base acceleration time history.

6 NUMERICAL MODEL

The employed time increment is 0.02 second which is much shorter than quarter of the smallest time period if earthquake. The deformed shape of mid-layer at starting time of failure is shown in Figure 3-a. Pore water pressure and effective mean stress contours at the starting time of instability are shown in Figures 3-b and 3-c, respectively. Zone including, the highest

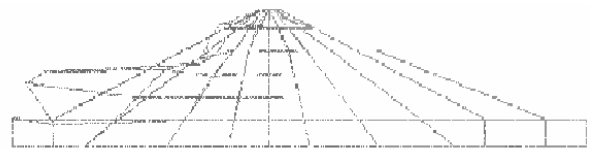


Figure 3 -a The deformed shape of mid layer

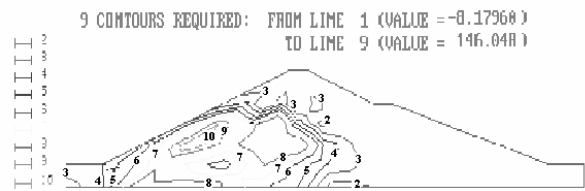


Figure 3 -b Built up pore water pressure



Figure 3 -c Effective mean stress contours

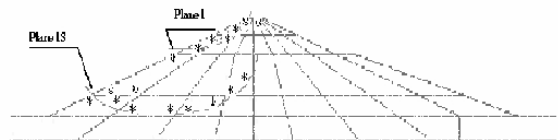


Figure 3 -d The failed Gauss points by shear

pore water pressure and negligible effective mean stress is the center where liquefaction was taken place Ishihara, et al. 1985. As this stage, first the liquefied zone started to move out of dam body and consequently, the upper part slid down. Some time

later post-seismic motion may have forced the slid particles to settle down and deform more. The ability of the multi-plane model and finite element developed program is to identify two forms of failure based on shear and tension of defined sampling planes. The identified plastic shear strain value for a failed plane is %15, and for tension is %5. Figure 3-d shows the failed gauss points to introduce the global form of collapsed band. Through the elements represented cohesive soil in core, plane number 2 of gauss point 8 of element number 87 tended to fail upon hydraulic fracture. The stress path, strain-stress, shear stress history, and the normal stress history of this plane are shown in Figure 4-a to 4-d, respectively. Figures 4-e to 4-g are the time histories for shear stress, normal stress, and pore water pressure on this plane. Figure 5 shows the failed gauss points by tension with the most probability of hydraulic fracturing.

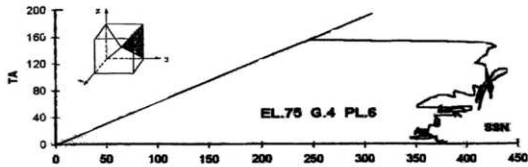


Figure 4-a Stress path on sheared plane

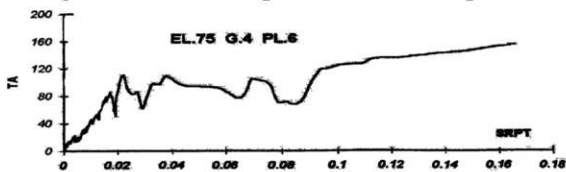


Figure 4-b Stress-Strain on Sheared plane

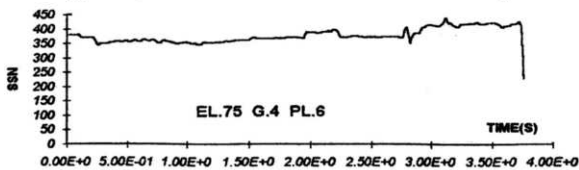


Figure 4-c Shear stress time history

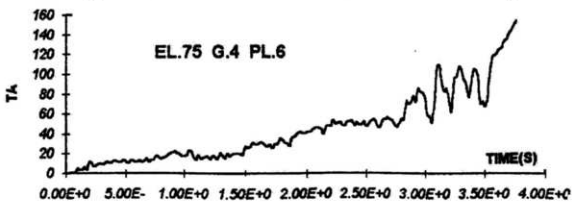


Figure 4-d Normal Stress time history

7 CONCLUSIONS

A unique model capable of predicting the behavior of both non-cohesive and cohesive, either in saturated or dry condition on the basis of sliding mechanisms, elastic behavior of particles and a higher effective hydrostatic pressure due to liquefaction in non-cohesive and hydraulic fracture in cohesive soil has been presented. The concept of multi-plane framework was applied successfully in dynamic analysis of three dimensional soil

structures. This is achieved by the use of a generally simplified, applicable, effective, and easily understandable relations between micro and macro scales. These relations demonstrate an easy way to handle any heterogeneous material property as well as mechanical behavior of materials. This, is actually, achieved in such a way that the application of some difficult tasks such as induced anisotropy and rotation of principal stress and strain axes where there is not coaxiality taking place during plastic flow, are out of constitutive relations. Accordingly, the sampling plane constitutive formulations provide convenient means to classify loading events, generate history rules and formulate independent evolution rules for local variables.

REFERENCES

- Zienkiewicz, O.C., and Pande, G.N., (1977), *Time dependent Multilaminar Model of Rocks*, Int. J. Num. Anal. Methods In Geomechanics, 1, 219-247.
- Pande, G.N. & Sharma, K.G., (1983), *Multilaminar model of clays-A numerical evaluation of the influence of rotation of principal stress axes*, Int. J. for Numerical and Analyt. Meth. in Geomech.
- Bazant Z.P. and Oh B.H., (1983), *Microplane model for fracture analysis of concrete structures*, Proceeding Symposium on the Interaction of Non-nuclear Munitions with Structures, held at US Air Force Academy, Colorado Springs, May 1983, Published by: McGregor & Werner, Washington DC.
- Pande G.N., and Pietruszczak, S., (1992), *Reflecting surface model for soils*, Proceeding International Symposium Numerical Methods in Geomechanics, Zurich, A.A. Balkema, Rotterdam, 50-64, 1982.5
- Sadrnezhad S.A., *Multilaminar elastoplastic model for granular media*, Journal of Engineering, Islamic Republic of Iran, vol.5, Nos.1&2, May, 1992-11
- Sadrnezhad, S.A. & Pande, G.N., (1989), *A Multilaminar Model For Sand*, Proceeding of 3rd International symposium on Numerical Models in Geomechanics, NUMOG-III, 8-11 May 1989, Niagara Falls, CANADA.
- Sadrnezhad S.A., (1999), *A Multilaminar Elastic-plastic Model For Liquefaction Of Saturated Sand*, Proceeding of the Third International Conference on Seismology and Earthquake Engineering, May 17-19, 1999, I.R.IRAN., p.561-568.
- Naylor, Stagg, and Zienkiewicz, (1975), *Numerical Analysis of Dams*, Swansae UCS publication.
- Lee, K.L., et al, (1975), *Properties of soil in the San Fernando hydraulic fill dams*, ASCE, Geotechnical Engineering Div., Vol. 101, pp.801-821.
- Seed, H.B., et al., (1975), *Dynamic Analysis of the slide in the lower San Fernando dam during earthquake of Feb. 9 1971*, ASCE, Geotechnical Engineering Div., Vol. 101, pp.889- 911.
- Seed, H.B., et al., (1975), *The slides in the San Fernando dam during earthquake of Feb. 9 1971*, ASCE, Geotechnical Engineering Div., Vol. 101, pp.651-685.
- Ishihara, *Liquefaction and flow failure during earthquakes*, Geotechnique, No.3, pp. 351-415.
- Pak, A. and Sadrnezhad, S.A., (1999), *Influence of initial effective principal stresses on hydraulic fracturing in soil*, Oct.1999, Scientia Iranica, Vol. 6, Nos. 3 & 4, pp 207-212, Sharif Univ. of Tech.
- Komakpanah A., et al, (1994), *Two dimensional study of hydraulic fracture criteria in cohesive soils*, Soil and Foundations, vol. 34, No. 1.
- Mederios et al., (1996), *A hydraulic fracturing test based on radial seepage in the Rowe consolidation cell*, In advances in site investigation practice, by Thames Telford, London.